

Iron and Sulfur Cycling in the Rhizosphere of Wild Rice (*Zizania palustris*)

A thesis
SUBMITTED TO FACULTY OF THE
UNIVERSITY OF MINNESOTA
BY

Sophia LaFond-Hudson

IN PARTIAL FULFILLMENT OF THE REQUIERMENTS FOR THE DEGREE OF
MASTER OF SCIENCE

Nathan Johnson, John Pastor

August 2016

Acknowledgements

I would like to acknowledge several people who contributed substantially to this project. The members of my committee, Dr. Nathan Johnson, Dr. John Pastor and Dr. Elizabeth Austin-Minor provided intellectual guidance during the experimental setup, data analysis, and writing process. Brad Dewey played an important role in this project by sampling the biological data, assisting with harvesting and cleaning roots, and answering question after question about the experimental setup and methods. Dan Fraser was likewise very helpful in answering any questions about equipment. I am very grateful for the help I received from Marissa Samuelson, who assisted considerably with geochemical sampling and cleaning roots. Finally, I would like to again thank my advisors, Dr. Johnson and Dr. Pastor, for being generous with their excellent advice and constant encouragement.

Abstract

Iron (hydr)oxides typically form on roots of many wetland plants, including wild rice (*Zizania palustris*), an annual macrophyte with significant cultural, economic, and ecological value. Iron (hydr)oxides are thought to protect macrophytes from toxic reduced species, such as sulfide, by providing an oxidized barrier around the roots. However, wild rice grown under high sulfate loading develops a black iron sulfide precipitate on the root surface, and produces fewer and lighter seeds, leading to a decreased population in the long term. In order to investigate the role of iron sulfide root precipitates in impaired seed production, wild rice plants grown in buckets were exposed to sulfate loading of 300 mg/L, and harvested biweekly for extraction of root acid volatile sulfide (AVS) and weak acid extractable iron and analysis of plant and seed N. In sulfate-amended plants, AVS on roots accumulated over the course of the growing season, and accumulated rapidly just prior to seed production. Simultaneously, iron speciation of the root precipitate shifted from Fe(III) to Fe(II), consistent with a transition from iron (hydr)oxide to iron sulfide. A mechanism is herein proposed by which sulfide-induced suberization of roots decreases radial oxygen loss that keeps the rhizosphere oxidized, leading to reduction of iron (hydr)oxides and subsequent iron sulfide accumulation. Plants amended with sulfate produced fewer, lighter seeds with less nitrogen. It is suggested that sulfide inhibits N uptake, and seeds are disproportionately harmed because rapid AVS accumulation occurs during the reproductive life stage.

Table of Contents

<i>List of tables</i>	<i>iv</i>
<i>List of figures</i>	<i>v</i>
<i>Introduction</i>	<i>1</i>
<i>Methods</i>	<i>4</i>
<i>Results</i>	<i>9</i>
<i>Discussion</i>	<i>19</i>
<i>Conclusion</i>	<i>24</i>
<i>References</i>	<i>26</i>
<i>Appendix</i>	<i>31</i>

List of Tables

Table 1 10

Appendix Table 1 31

List of Figures

<i>Figure 1</i>	<i>11</i>
<i>Figure 2</i>	<i>14</i>
<i>Figure 3</i>	<i>15</i>
<i>Figure 4</i>	<i>18</i>
<i>Figure 5</i>	<i>20</i>
<i>Appendix Figure 1</i>	<i>31</i>
<i>Appendix Figure 2</i>	<i>32</i>
<i>Appendix Figure 3</i>	<i>32</i>

Introduction

Iron (hydr)oxide plaques have been observed on the roots of wild rice (*Zizania palustris*), a culturally significant macrophyte that forms large monotypic stands in the lakes and rivers of Minnesota, Wisconsin, northern Michigan, and Ontario (Lee and McNaughton 2004, Jorgenson et al. 2013). Iron (hydr)oxide plaques commonly form on the roots of wetland plants growing in anoxic, reduced sediments as a result of a redox gradient found in the rooting zone (Mendelssohn and Postek 1982, Jacq et al. 1991, Snowden and Wheeler 1995, Christensen and Sand-Jensen 1998). Redox gradients in the rhizosphere are caused by radial oxygen loss, a process in which wetland plants release oxygen into the rhizosphere through their roots via aerenchyma tissue (Armstrong and Armstrong 2005, Schmidt et al. 2011). When Fe(II) is transported from anoxic sediment into the oxygenated rhizosphere, it is oxidized to Fe(III), which combines with oxygen from the roots to form insoluble iron oxides or hydroxides. Iron plaque formation can occur abiotically, but it is also associated with iron-oxidizing bacteria in many cases (St. Cyr 1993, Neubauer et al. 2007). Iron plaques have been proposed as a mechanism to protect plants from reduced toxic substances such as hydrogen sulfide, because they form an oxidized barrier around the roots (Koch and Mendelssohn 1989, Mendelssohn et al. 1995). However, during previous sulfur addition experiments, black iron sulfide root coatings, characteristic of iron sulfide minerals, have been observed on wild rice roots (Pastor et al., in review). Black root coatings have also been observed in white rice grown in surface water with high sulfate concentrations (Jacq et al. 1991, Gao et al. 2003, Sun et al. 2015).

The iron and sulfur chemistry of aquatic plant rooting zones involves a set of interrelated biogeochemical processes. Sulfate and iron (III) oxides are both redox active species that play a role in degradation of organic matter in aquatic sediments. During aerobic respiration, electrons are transferred from organic compounds to oxygen, but in anaerobic respiration alternative electron acceptors are used, including nitrate, ferric iron, sulfate, and carbon dioxide. Organisms use the more thermodynamically favorable electron acceptors first; nitrate is used before ferric iron, and carbon dioxide is used only when more favorable electron acceptors have been consumed. This thermodynamic ordering manifests itself as stratified microbial communities with distance away from an

oxic-anoxic boundary (Boudreau 1996, Van Cappellen and Wang 1996). Anaerobic respiration produces reactive reduced species as byproducts, including ammonia, ferrous iron, sulfide, and methane. Iron-reducing and sulfate-reducing bacteria facilitate production of ferrous iron and sulfide respectively, after which ferrous iron and sulfide can combine to produce iron monosulfide (FeS) or pyrite (FeS₂). Alternatively, ferrous iron and sulfide can undergo oxidization back to ferric iron and sulfate abiotically via bioturbation or water level fluctuations (Thamdrup et al. 1994, Eimers et al. 2003) or biotically via iron or sulfide oxidizing bacteria (lithoautotrophy). Despite the predictability of the sequence of electron acceptors used in anaerobic respiration, coincident iron reduction and sulfate reduction in close proximity has been documented, during which the subsequently produced sulfide reacts abiotically with nearby iron (hydr)oxides to produce reduced iron and elemental sulfur (Hansel et al. 2014, Kwon et al. 2013).

Macrophytes can accelerate iron and sulfur cycling by enhancing redox gradients when radial oxygen loss creates an oxic layer around the root surface. Oxidation of Fe(II) to Fe(III) oxides immobilizes iron on or very near the root surface. Conversely, oxidation of sediment FeS by radial oxygen loss mobilizes previously bound sulfur as soluble sulfate (Choi et al. 2006). Cycling is dynamic near the rhizosphere because oxidation potential (Eh) changes abruptly over just a few millimeters. Just outside the oxic layer, the sediment can be strongly reducing. Heterotrophic iron and sulfate reduction can be stimulated by root exudates released by the plant (Kimura et al., 1981), and, in the case of an annual plant like wild rice, senesced plant material at the end of the growing season each year (Jacq et al. 1991). Several studies have compared sediment with and without vegetation and found higher sulfide or FeS concentrations in sites with plants (Holmer and Nielsen, 1997, Jacq et al. 1991, Lee and Dunton 2000). The increase in reduced species is attributed to larger pools of organic matter to drive reduction.

In Minnesota, surface water sulfate concentrations are regulated in wild rice waters because high surface water sulfate concentrations are associated with decreased wild rice abundance (Moyle, 1945, MPCA Analysis of the Wild Rice Sulfate Standard Study, 2014). It has recently been shown that sulfide, the reduced form of sulfur, is toxic to wild rice seedlings (Pastor et al., in review). In other wetland plants, sulfide is thought

to interrupt metabolism by inhibiting metallo-enzymes in the electron transport chain during respiration (Allam and Hollis 1972, Koch and Mendelssohn 1989, Koch et al. 1990, Lamers et al. 2013; Armstrong and Armstrong 2005, Martin and Maricle 2015). Inhibition of ATP production deprives a plant of energy required for nutrient uptake. Sulfide has been shown to reduce nutrient uptake in white rice (*Oryza sativa*), a plant physiologically similar to wild rice (Joshi et al. 1975), so it is plausible that sulfide may also inhibit nutrient uptake in wild rice.

Pastor et al. (in review) found that exposure to sulfide slightly decreased plant biomass, and markedly decreased mean seed weight and the proportion of filled seeds. Wild rice takes up nitrogen, its limiting nutrient, in three main bursts: 30% is taken up during early season vegetative growth, 50% is taken up during early flowering, and 20% is taken up during late flowering and seed production (Grava and Raisanen, 1978). The effects of sulfide exposure on wild rice are consistent with nitrogen limitation during seed production, but it is not well understood why the seed production life stage is disproportionately harmed by sulfide. Is iron sulfide plaque accumulation a geochemical mechanism that controls the impact of sulfide on nitrogen uptake?

The objective of this study is to understand how iron and sulfur cycle near root surfaces and how this cycling affects nitrogen uptake by wild rice during its life stages, especially seed production. We investigate the drivers of iron sulfide plaque formation and seek to answer if plant and seed nitrogen uptake are adversely affected by iron sulfide accumulation on root surfaces.

Methods

Experimental Design

Sediment was collected from Rice Portage Lake (MN Lake ID 09003700, 46.703810, -92.682921) on the Fond du Lac Band of Lake Superior Chippewa Reservation in Carlton County, Minnesota in late May, 2015 and placed in a 400 L Rubbermaid stock tank where it was homogenized by shovel. Initial carbon in the sediment was 14.8 ± 1.70 % and initial nitrogen was 1.12 ± 0.13 % by dry weight. Eighty 4 L plastic pails were then filled with 3 L of the sediment. Each 4 L pail was placed inside of a 20 L bucket which was filled with 12 L of water to provide a 12-15 cm water column. The overlying water of 40 randomly chosen buckets was then amended with an aliquot of stock solution (5.15 g of Na_2SO_4 dissolved in 200 ml of deionized water) to result in 300 mg/L (3.125 mM) sodium sulfate. The amendment concentration was chosen as such because when used in previous mesocosm experiments, wild rice populations went extinct within five years (Pastor et al. in review), but it is only slightly higher than the EPA drinking water secondary standard (250 mg/L) and is a concentration found in some Minnesota lakes (MPCA Analysis of the Wild Rice Sulfate Standard Study, 2014). The overlying water was sampled twice throughout the trial and re-adjusted to 300 mg/L SO_4 by adding additional Na_2SO_4 stock solution. The other 40 buckets did not receive any sulfate and on 6/23/15 (day 174, Julian date) had an average surface water sulfate concentration of 14.44 ± 1.01 mg/L, consistent with the local groundwater sulfate concentration. In each bucket, two seeds which were harvested in 2014 from Swamp Lake on the Grand Portage Reservation (MN Lake ID 16000900, 47.951856, -89.856844) were planted on 5/15/15 (Julian day 135). Once shoots reached a height of approximately 20 cm during the aerial stage, plants were thinned to one plant per bucket.

Sampling of pore water, roots, and stems began midsummer (63 days after planting/germination), at the start of flowering and the second burst of nitrogen uptake (Grava and Raisanen, 1978), and continued until plants had thoroughly senesced, for a total of eight sample dates, not including initial sediment and pore water sampling. Sampling occurred every two weeks for the first four sample dates, (flowering, days 189-232) and weekly for the last four sample dates (seed production, days 238-265), for a

total of eight sample dates. One week prior to each sampling date, 40 ml of enriched ^{15}N solution were injected into the sediment of four randomly selected sulfate-amended buckets and four control buckets. For the first two sample dates, the labeling solution was prepared by adding 0.88 mg of 10% $^{15}\text{N-NH}_4\text{Cl}$ to 500 ml DI water. For all other sample dates, 2.2 mg of 10% $^{15}\text{N-NH}_4\text{Cl}$ were added to 500 ml of DI water to account for an increase in plant biomass later in the growing season. The solution was injected into the sediment of the 4 L pail in four locations uniformly spaced around the center of the pail, approximately 2 cm from the outer edge and 2 cm from the bottom. Immediately before injection, the overlying water was removed from the outer pail, leaving 2-5 cm above the sediment in the internal pail, to keep the $^{15}\text{N-NH}_4\text{Cl}$ contained in the sediment for uptake by the wild rice roots. On each sample date, one week after injection of ^{15}N , the four sulfate-amended and four control buckets were sampled for pore water sulfide, pore water sulfate, pore water iron, and pH. After pore water sampling, the wild rice plant was destructively harvested for analysis of vegetative ^{15}N , vegetative total N, and root AVS and weak acid extractable iron. The bulk sediment was sampled for solid phase S and Fe analysis at the beginning and at the end of the growing season.

Pore water sampling and analysis

Prior to extracting pore water samples, pH was measured *in-situ* with a ThermoScientific Orion pH electrode at a depth of 5 cm below the sediment surface and 2 cm from the stem of the wild rice plant. Pore water was sampled using 5-cm length, 2-mm diameter tension lysimeter filters (Rhizons, Seeberg-Elverfeldt et al., 2005) attached with a hypodermic needle to an evacuated, oxygen-free serum bottle sealed with a 20 mm thick butyl-rubber stopper (Bellco Glass, Inc). The entire filter end of the Rhizon was inserted vertically into the sediment just below the surface. The goal was to draw water from approximately the upper 5 cm of sediment without drawing surface water. The filter was placed with minimal jostling to avoid creating a cavity around the filter that would allow surface water to enter the sediment and contaminate the pore water. The Rhizon was placed approximately 2 cm away from the stem of the wild rice plant and on the opposite side from where pH was measured.

Pore water sulfide samples were drawn into 50-mL serum bottles preloaded with 0.2% 1 M ZnAc and 0.2% 6 M NaOH to preserve sulfide. Sulfide bottles were left to fill

overnight, then stored at 4C in the sealed serum bottles used for sample collection for approximately 30 days before sulfide was quantified. Samples for pore water sulfate analysis were withdrawn from sulfide sampling bottles and filtered through a Dionex 1cc metal cartridge and a 0.45 μm polyethersulfone filter approximately three months after they were collected. Pore water iron was collected in 8-mL serum bottles preloaded with 40% deionized water, 40% phenanthroline, 20% acetate buffer, and 1% concentrated hydrochloric acid. Iron bottles were filled until the solution turned light red, approximately ten minutes. If the solution turned red before 8 mL were collected, samples were diluted with deionized water to bring the total solution to 8 mL. Iron samples were quantified within two hours of sampling. Iron and sulfide were quantified colorimetrically using the phenanthroline and methylene blue methods, respectively, on a HACH DR5000 UV-Vis spectrophotometer (Eaton et al., 2005). Sulfate was quantified using a Dionex ICS-1100 Integrated IC system (AS-DV Autosampler) (Eaton et al., 2005).

Solid phase sampling and analysis

Samples for the bulk sediment initial conditions were obtained after homogenization of the sediment prior to placement in the buckets (day 152). Five replicate samples were placed in jars and analyzed for AVS and simultaneously extracted iron. At the end of the season, mini-cores of intact sediment were retrieved immediately before wild rice plants were sampled.

On each sample date throughout the summer, wild rice roots were collected for AVS and weak acid extractable iron. Each plant was removed from the sediment and immediately rinsed in buckets of deoxygenated water continuously bubbled with nitrogen. While submerged in deoxygenated water, the stem was cut just above the root ball so that the shoots and any seeds could be saved for ^{15}N analysis. Roots were then placed in jars full of deoxygenated water, which were immediately placed in a plastic bag flushed with nitrogen and transported to an oxygen-free glove box. In the glove box, the roots were cleaned of extra organic matter prior to removing a 1-2 g section of wet root mass for AVS and iron analysis. From both sediment and roots, AVS was extracted using 7.5 ml 1 N HCl for 4 hours using a modified diffusion method (Brouwer and Murphy 1994). During a room temperature acid incubation with gentle mixing, sulfide

was trapped in an inner vial containing Sulfide Antioxidant Buffer (SAOB) and subsequently quantified using a ThermoScientific sulfide ion-selective electrode with a detection limit ranging from 0.01-40 mmol/L. Ferrous iron was quantified colorimetrically using the phenanthroline method on a HACH DR5000 UV-Vis spectrophotometer (Eaton et al., 2005), and weak acid extractable iron was quantified using a Varian fast sequential flame atomic absorption spectrometer with an acetylene torch.

A subset of roots was tested for chromium(II)-reducible sulfur (CRS) to determine whether AVS was extracting all total reduced inorganic sulfur on the roots. A diffusion-based CRS method was used, which can fully extract amorphous iron sulfide and pyrite and can partially extract elemental sulfur (Burton et al. 2008). Chromic acid for CRS analysis was prepared according to Burton et al. (2008). Inside an oxygen-free glove box, a section of root from a plant previously analyzed for AVS was placed in the analysis bottle. An inner vial containing SAOB was also placed inside the bottle prior to sealing. Bottles were taken out of the glove box and injected with chromic acid. CRS was extracted for 48 hours and quantified using a ThermoScientific sulfide ion-selective electrode.

Isotope sampling and analysis

For analysis of ^{15}N uptake, the plants were sub-sampled by cutting at the stem to root transition. If seeds were present, they were removed prior to sampling the plant and saved for separate analysis. The plants and seeds were rinsed with deionized water and dried in paper bags for seven days at 65 °C. The dried plants were weighed, placed in polycarbonate vials with stainless steel balls, and shaken in a SPEX 800M mixer mill until the samples were in a powdered form. Seeds were counted, weighed, and powdered using the same method. The samples were transferred to glass vials and dried again overnight at 65 °C with caps loosely covering the vials. Samples were quantified for total N and $\delta^{15}\text{N}$ on a Finnigan Delta Plus XP isotope ratio monitoring mass spectrometer.

Data analysis

Geochemical parameters and measured attributes of plants were analyzed using repeated measures analysis of variance to determine differences between sulfate

amendments and controls. A paired *t* test was used to determine differences between AVS and CRS concentrations on roots. A two-factor ANOVA was used to compare pre-planting and post-senescence sediment concentrations of iron and AVS between treatments. Analyses were performed using the statistical software SAS. Logarithmic transformations were used when data was non-normal. A reciprocal transformation was used for dry weight of plants, as a logarithmic transformation was not effective. Data for root AVS were split into pre-seed production and post-seed production because the full-season data was not able to be transformed.

The saturation index was calculated to determine if the pore water was saturated enough to precipitate iron sulfide (equation 1). A positive saturation index value indicates precipitation, and a negative value indicates dissolution. The K_{sp} value used was $10^{-2.95}$ (Stumm and Morgan, 1995).

$$SI = \log \frac{[IAP]}{K_{sp}} \text{ where } IAP = \frac{[Fe^{2+}][HS^{-}]}{[H^{+}]} \quad \text{Equation 1}$$

Changes in the accumulation rates of root AVS and ferrous iron were tested by fitting linear regressions to the concentrations of root AVS and Fe^{2+} prior to seed production (days 189-231). The model was extrapolated to late season sample dates (days 232-264) to test if accumulation rates changed between flowering and seed production.

A mixing model was used to determine the proportion of seed nitrogen originating from the pore water and the proportion translocated from the stems (equations 2 and 3). The $\delta^{15}N$ of the seeds was measured, and the $\delta^{15}N$ of the pore water and the stems were approximated. The plant $\delta^{15}N$ was estimated to be 4.5‰ from the average of 12 unlabeled plants harvested on the first two sample dates. The pore water $\delta^{15}N$ was approximated to be 180‰ and calculated from the percent by mass of $^{15}NH_4$ added ($\delta^{15}N = 26,200‰$) and the percent by mass of ammonia already present in the pore water ($\delta^{15}N$ assumed to be 0‰). In equation 2, δ_{sample} is the isotopic signature of nitrogen in the seed, δ_{source1} is the isotopic signature of the pore water ammonium, f_1 is the proportion of nitrogen coming from the pore water, δ_{source2} is the isotopic signature of nitrogen in the plant stem, and f_2 is the proportion of the nitrogen sourced from the plant stem. Seed

nitrogen can be sourced only from the pore water or the stems, so the proportions from both components must sum to one (equation 3).

$$\delta_{sample} = \delta_{source1} \times f_1 + \delta_{source2} \times f_2 \quad \text{Equation 2}$$

$$f_1 + f_2 = 1 \quad \text{Equation 3}$$

Results

Pore water

Although sulfate was 40x higher in the overlying water of sulfate-amended plants, pore water sulfide concentrations were only approximately twice as high in the in the rooting zone of sulfate-amended plants compared to the control over the entire growing season. Sulfide concentration and variability increased in the pore water of both amended and control rooting zones one week after the first seeds were produced (day 238, Julian date) and returned to initial concentrations two weeks later (day 245, Fig. 1a). Pore water sulfide data did not fit any parametric model, so a repeated measures ANOVA was not performed.

Pore water iron concentrations were not correlated with sulfate amendment (Table 1). Pore water iron decreased until shortly after seed production began (day 238) in both amendments. The minimum iron concentration occurred at the same time that a peak in pore water sulfide developed (Fig 1b). Shortly before senescence (days 252 and 264), the iron concentrations returned to values similar to concentrations during the first month of data collection.

The pore water pH and saturation index were not correlated with sulfate amendment (Table 1). The pH of the pore water peaked at the start of seed production (days 231-238, Fig.1c). This peak occurred approximately one week before the iron minimum and the sulfide maximum. The saturation index peaked one week after the first seeds were produced, when pH and sulfide were elevated and iron was low (day 238, Appendix Table 1). The average saturation index was above zero only in the sulfate-amended buckets on day 238. The saturation index gradually declined for the rest of the growing season.

Sulfate concentrations ranged from 10-30 times higher in the pore water of plants amended with sulfate (Table 1). Sulfate increased in the amended pore water until seed production began, when it declined precipitously from 2300 $\mu\text{mol/L}$ to 770 $\mu\text{mol/L}$ over 15 days (Fig 1d). In the pore water of control plants, sulfate concentrations followed a similar trend, but at lower concentrations. Control sulfate peaked at 230 $\mu\text{mol/L}$ before decreasing to 34 $\mu\text{mol/L}$. Sulfate declined just prior to an increase in pore water sulfide.

Table 1. Results of repeated measures ANOVA testing effect of sulfate, time and interaction of sulfate and time on geochemical and biological variables. Tests for pore water and root parameters include data from the entire growing season, whereas tests for biological parameters only include data from mature seed production. *F* values and degrees of freedom (*d.f.*) are given. Tests for time and sulfate x time have the same number of degrees of freedom. Significance levels are shown using asterisks (***) indicates $p < 0.001$, ** indicates $0.001 < p < 0.05$, * indicates $0.05 < p < 0.10$).

Repeated measures ANOVA (F values)			Sulfate	d.f.	Time	Sulfate x Time	d.f.
Pore water geochemistry							
Iron	5.16	1, 5	5.51***	1.14	6, 35		
pH	3.25	1, 6	12.5***	1.45	6, 36		
Saturation index	2.68	1, 4	2.19*	0.50	6, 34		
Sulfate	239***	1, 3	8.17***	1.09	5, 27		
Root geochemistry							
AVS (during flowering)	66.1***	1, 5	1.10	0.40	3, 17		
AVS (during seed production)	148***	1, 6	5.46**	1.76	4, 24		
Weak acid extractable iron	0.53	1, 6	2.65	2.42**	7, 42		
Ferrous Iron	127***	1, 6	57.2***	3.34**	6, 36		
% Ferrous Iron	235***	1, 6	41.5***	4.91***	6, 36		
Biological variables (during seed maturity)							
Plant N (total mass)	1.53	1, 6	0.35	0.25	2, 12		
Plant weight	5.00*	1, 6	0.40	0.31	3, 18		
Seed N (total mass)	5.84*	1, 6	1.10	1.22	2, 12		
Seed weight	4.88*	1, 6	0.59	0.94	2, 12		
Seed count	5.00*	1, 6	1.89	0.70	2, 12		
Seed $\delta^{15}\text{N}$	1.47	1, 6	2.45	0.05	2, 12		
Seed N%	1.70	1, 6	3.04*	0.40	2, 12		
Vegetative N (plant+seed mass)	5.43*	1, 6	0.32	1.71	2, 12		

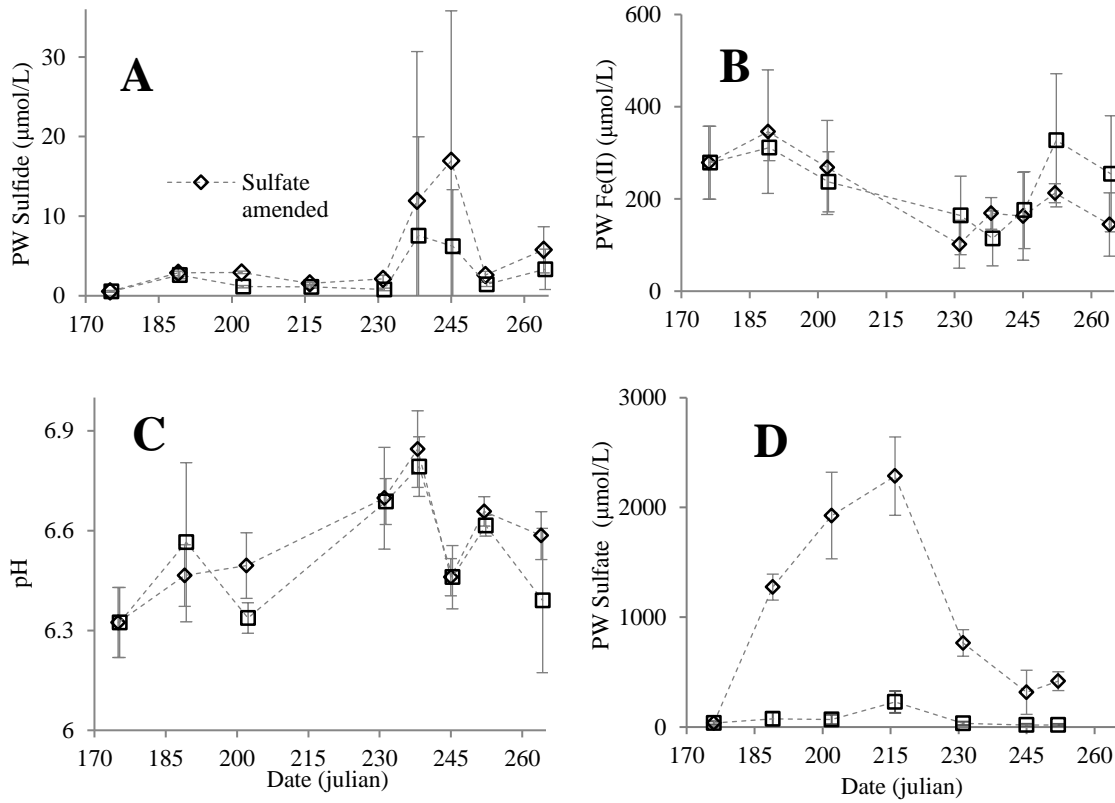


Figure 1. Pore water (PW) data measured in buckets during summer of 2015. Diamonds indicate data from buckets amended with 300 mg/L sulfate. Squares represent data from control buckets. Time is shown in Julian days. Error bars indicate one standard deviation. Control data points are slightly offset to show overlap in error bars.

Roots

Wild rice plants grown in sediment with high overlying water sulfate concentrations developed a black coating on their root surfaces (Appendix Fig. 1). A SEM scan of the roots showed that the root precipitate contained iron and sulfur in approximately a 1:1 ratio (Dan Jones, unpublished data). The oxic/anoxic interface was often recorded on the root; the black coating started on the stem just above the root ball and extended downwards along the entire length of the roots. Adventitious roots that grew at the surface of the sediment remained white, the natural color of wild rice root tissue. Control plants, grown in sediment with low overlying water sulfate, formed very little black color on their roots, instead appearing amber, a color characteristic of iron (hydr)oxides.

Roots grown under elevated sulfate (hereafter “amended roots”) accumulated AVS concentrations up to two orders of magnitude higher than the control roots by late summer. Amended root AVS peaked at 298 ± 74 $\mu\text{mol/g dw}$ immediately prior to senescence (Fig 2a). Concentrations of AVS on roots grown under control surface water sulfate (hereafter “control roots”) did not consistently increase, and averaged of 3.2 ± 1.7 $\mu\text{mol/g dw}$. For amended roots, the rate of accumulation of root AVS appeared relatively constant (linear) until the first day seeds were produced (day 232), when the rate of AVS accumulation appeared to increase abruptly. During seed production, AVS concentrations were greater than that predicted by a linear model (constant accumulation rate), suggesting that the net rate of AVS accumulation on amended roots increased rapidly when seed production began. Points after the first day of seed production (day 231) fell outside of a 95% CI of a linear regression on the points during flowering (days 190-231, Appendix Fig. 2). Concentrations of CRS on both amended and control roots did not differ from AVS concentrations on the same roots, indicating that crystalline forms of FeS did not make up a significant proportion of reduced sulfur (paired *t* test, $p=0.27$, $t=0.63$, $n=20$).

Ferrous iron accumulation paralleled AVS accumulation on amended roots (Fig 2b). Root ferrous iron concentrations were elevated and accumulated faster on the amended roots compared to the control (Table 1). Ferrous iron on control roots and amended roots increased linearly, but ferrous iron on amended roots increased at a higher

rate until the first seeds were produced (day 232). During seed production, ferrous iron concentrations on amended roots were greater than those predicted by a linear model, while Fe(II) accumulation on control roots appeared to slow.

Weak acid extractable iron (sum of Fe(II) + Fe(III) concentrations on roots, hereafter “total extractable iron”) was variable, but did not differ significantly between treatments (Table 1). The average total extractable iron remained relatively constant in both treatments during flowering; however, during the first week of seed production (days 232 and 239) the total extractable iron dropped by about 150-250 $\mu\text{mol/g}$ on both the amended and control roots, and then gradually increased over the following three weeks (Fig. 3). Total extractable iron changed seasonally from mostly Fe(III) to mostly Fe(II) on sulfate-amended roots, especially during the first week of seed production (days 232 and 239). This abrupt shift in iron speciation occurred the same week that total extractable iron decreased and at about the same time as the increase in AVS accumulation rate (Fig. 3). Immediately prior to seed production, total extractable iron on the amended roots was $46 \pm 11\%$ Fe(II), and after one week of seed production, the composition of iron was $87 \pm 10\%$ Fe (II). During this same week, the percentage of total extractable iron that was Fe(II) on control roots increased from $20 \pm 11\%$ to $48 \pm 16\%$.

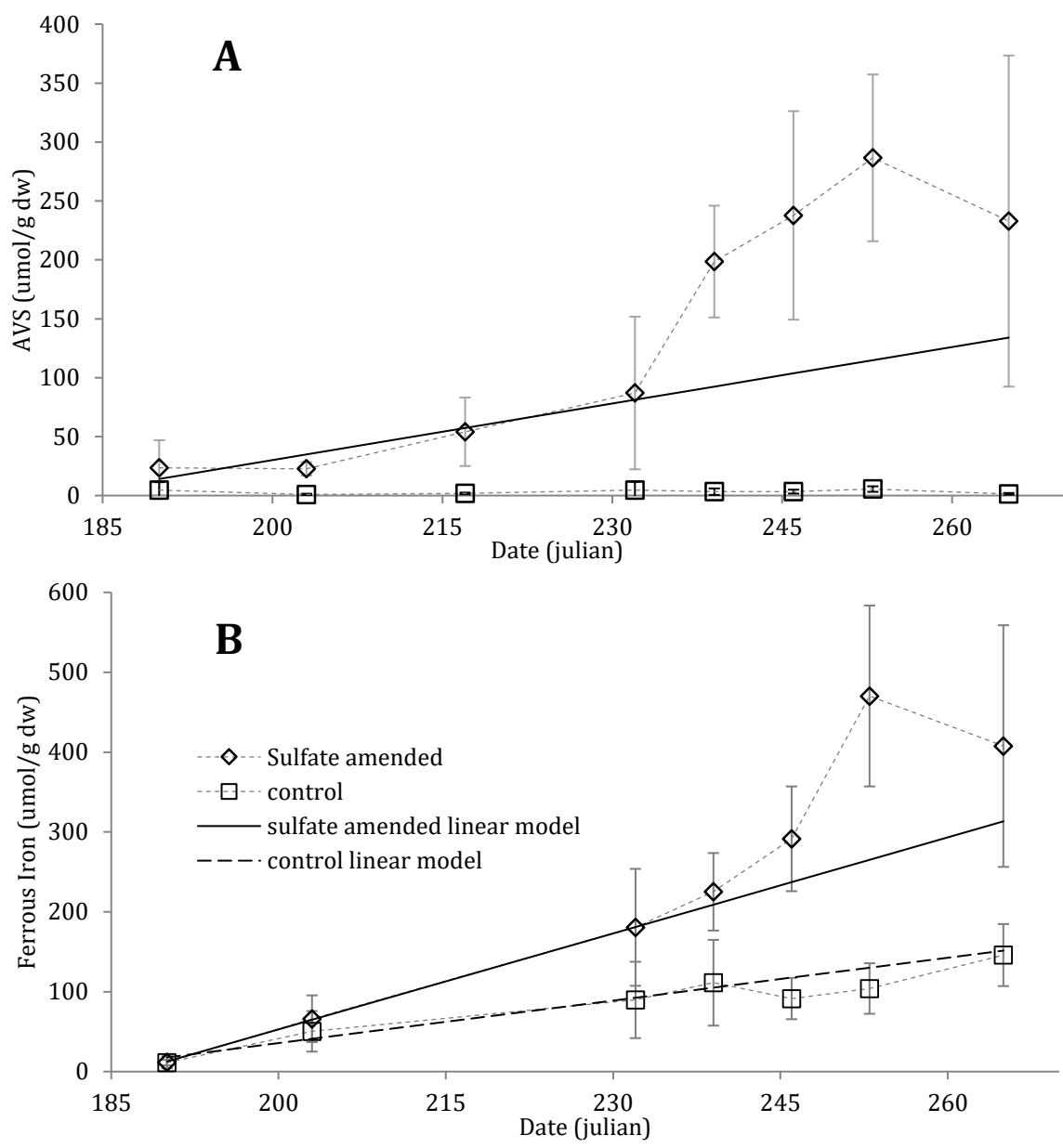


Figure 2. Solid phase acid volatile sulfide (A) and ferrous iron (B) concentrations on roots. Diamonds represent the average concentration on roots of four sulfate-amended plants, and squares represent the average of four control plants. The dashed line shows a linear model fit to the data from day 190 to day 232. Time is expressed in Julian dates. Error bars show one standard deviation.

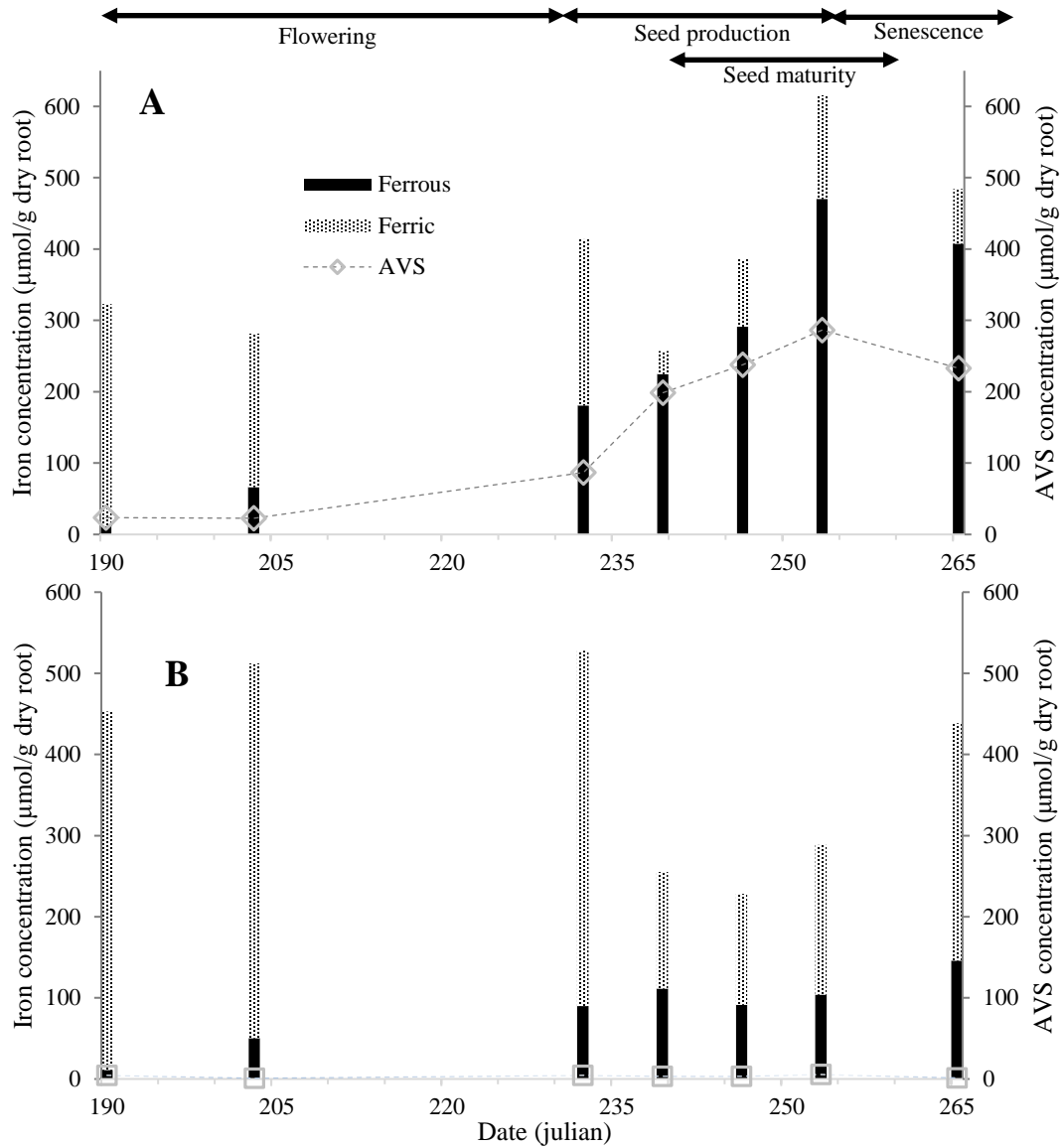


Figure 3. Seasonal iron speciation with root AVS overlain in sulfate-amended bucket. The dotted pattern indicates ferric iron and the solid black represents ferrous iron. A). Sulfate-amended bucket iron. Grey diamonds show root AVS concentrations in sulfate-amended buckets. B). Control bucket iron. Grey squares show root AVS concentrations in control buckets. Error bars are omitted for clarity.

Sediment

Sediment AVS was significantly different between treatments, but total extractable iron was not. In both the sulfate-amended and control sediment, AVS increased during the growing season, but more AVS accumulated in the amended sediment (2-factor ANOVA, time x treatment interaction, $f=5.08$, $df=1,18$, $p=0.037$). Amended sediment AVS increased from 0.39 $\mu\text{mol/g}$ in early summer to 4.7 $\mu\text{mol/g}$ at the end of the growing season, whereas the control sediment only increased from 0.39 $\mu\text{mol/g}$ to 0.88 $\mu\text{mol/g}$. There was no difference in total extractable iron between the amended and control sediment at the beginning or end of the growing season (2-factor ANOVA, $f=0.65$, $df=1,18$, $p=0.429$).

Biological effects

Plant sampling began at the start of the flowering stage (days 190-230). The first seeds were collected on 8/20/15 (day 232), but were unripe and not yet filled. In this paper, seed production is referred to as days 230 to day 264, but mature seeds were not produced until one week after the start of seed production (day 239). On the last sample date (day 265) seeds were collected, but were unfilled. Stems and leaves were no longer green, indicating that the plants had senesced. Of the four replicates in the sulfate amendment on this date, two plants did not produce seeds. Thus, “mature seed production” refers to dates 239-253.

Total seed nitrogen, total seed weight, and seed count were all lower in sulfate-amended plants during mature seed production, a time that coincided with elevated FeS on roots (days 239-253, Table 1, Fig 4). Sulfate addition was not correlated with seed $\delta^{15}\text{N}$ or seed N %. During mature seed production and senescence, the dry weight of the sulfate-amended plants was lower than that of control plants. Total vegetative (plant + seeds) N was unaffected by sulfate until the last two sample dates prior to senescence, when it was lower in sulfate-amended plants (Fig 4d, two-sample t test, $p=0.031$, $p=0.047$, $n=8$ for both dates).

A mixing model was used to determine the fraction of total seed nitrogen coming from the pore water and the fraction translocated from the stem (Appendix Fig. 3). In the days following a spike of enriched nitrogen to sediment pore water, there were two possible sources of nitrogen in the seeds; wild rice can translocate nitrogen from its stem

or take nitrogen up from the pore water. The two-component mixing model showed no difference in fraction of nitrogen uptake from pore water between the amended and control plants (repeated measures ANOVA, $p=0.83$, $f=0.05$, $df=1,6$). In both control and amended plants, the fraction of total seed nitrogen originating from the pore water increased two weeks into seed production (day 246) from $27 \pm 18\%$ to $51 \pm 19\%$, but returned to $29 \pm 19\%$ a week later (day 253). The elevated proportion coming from the pore water coincides with the day seeds contained the most nitrogen (Fig 4c). On this day, total seed nitrogen was significantly lower in the sulfate amended plants than in the control plants (two-sample t test, $p=0.047$, $n=8$). Plant N (excluding seeds), however, was not different between amended and control plants on this day (two-sample t test, $p=0.41$, $n=8$).

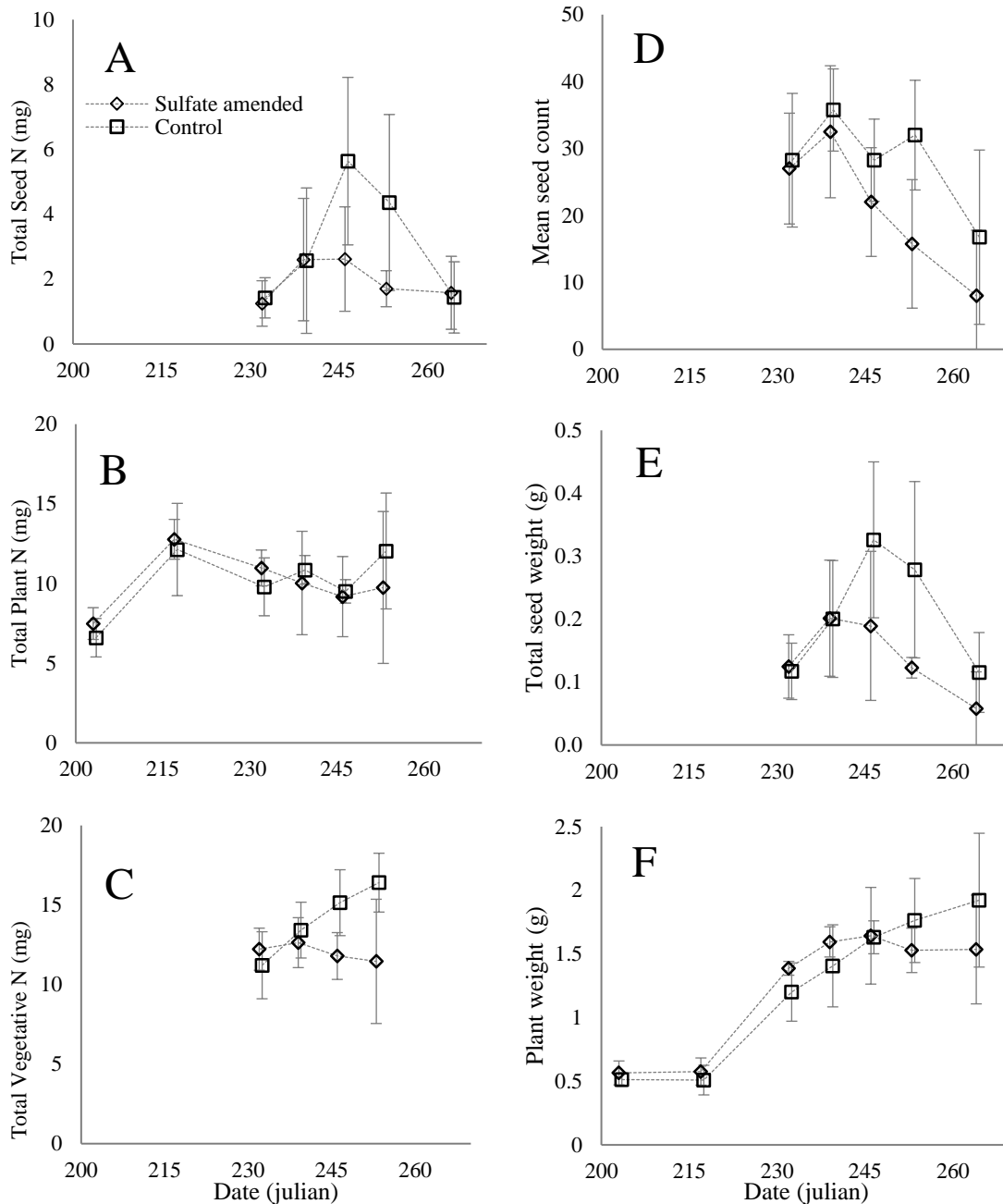


Figure 4. Biological endpoints. Diamonds represent plants grown in surface water with 300 mg/L sulfate added while squares show data from control plants. Each data point represents four replicates. Error bars represent one standard deviation. A) Weekly total mass of nitrogen in seeds of sulfate amended and control plants. B) Total mass of nitrogen in the plant (stems+leaves), excluding seeds, over the course of the growing season. C) Weekly total vegetative nitrogen in amended and control plants. Total vegetative nitrogen was calculated by summing nitrogen from seeds, stems, and leaves. D) Weekly seed count in amended plants and control plants. E) Weekly total seed mass in amended plants and control plants. F) Dry mass of plants over the course of the growing season.

Discussion

Our observations suggest a tight coupling of iron and sulfur cycling in the rooting zone of wild rice. Iron (hydr)oxides form on wild rice roots early in the growing season, but roots that are exposed to high sulfate loading (300 mg/L) develop iron sulfides later in the growing season. An inflection point in iron sulfide accumulation occurs at the start of seed production, shortly after rapid depletion of sulfate in the pore water, and defines an increase in the net rate of FeS accumulation. The rapid increase in net FeS accumulation suggests a change in a process that controls the way iron and sulfur cycle in the rhizosphere, and the timing suggests that this process may be tied to and have important implications for rice physiology. Previous research has suggested that an accumulation of FeS occurs after plant senescence (Jacq 1991), but our observations clearly show accumulation of FeS during the reproductive life stage of wild rice.

The change in FeS accumulation rate is consistent with an inhibition of radial oxygen loss. Sulfate accumulation in the pore water during the flowering stage suggests that the rhizosphere is relatively oxidized. The initially linear FeS accumulation rate on plant roots suggests constant rates of sulfide production and sulfide oxidation, with a higher rate of sulfide production than oxidization (net accumulation). However, sulfide exposure in white rice leads to the formation of suberin in the cell walls of roots which is hypothesized to create a barrier that limits diffusion of toxic solutes into the plant (Armstrong and Armstrong, 2005). The barrier not only excludes toxic solutes like sulfide, but also traps oxygen inside the roots, suppressing radial oxygen loss (Krishnamurthy et al. 2009, Soukup et al. 2006). A relatively rapid transition to anoxia of the rhizosphere appears to have occurred at the onset of seed production, possibly as a result of suberin-induced suppression of radial oxygen loss. Under the anoxic conditions, the net accumulation of reduced species likely increased because fewer reduced species cycled back to their oxidized form.

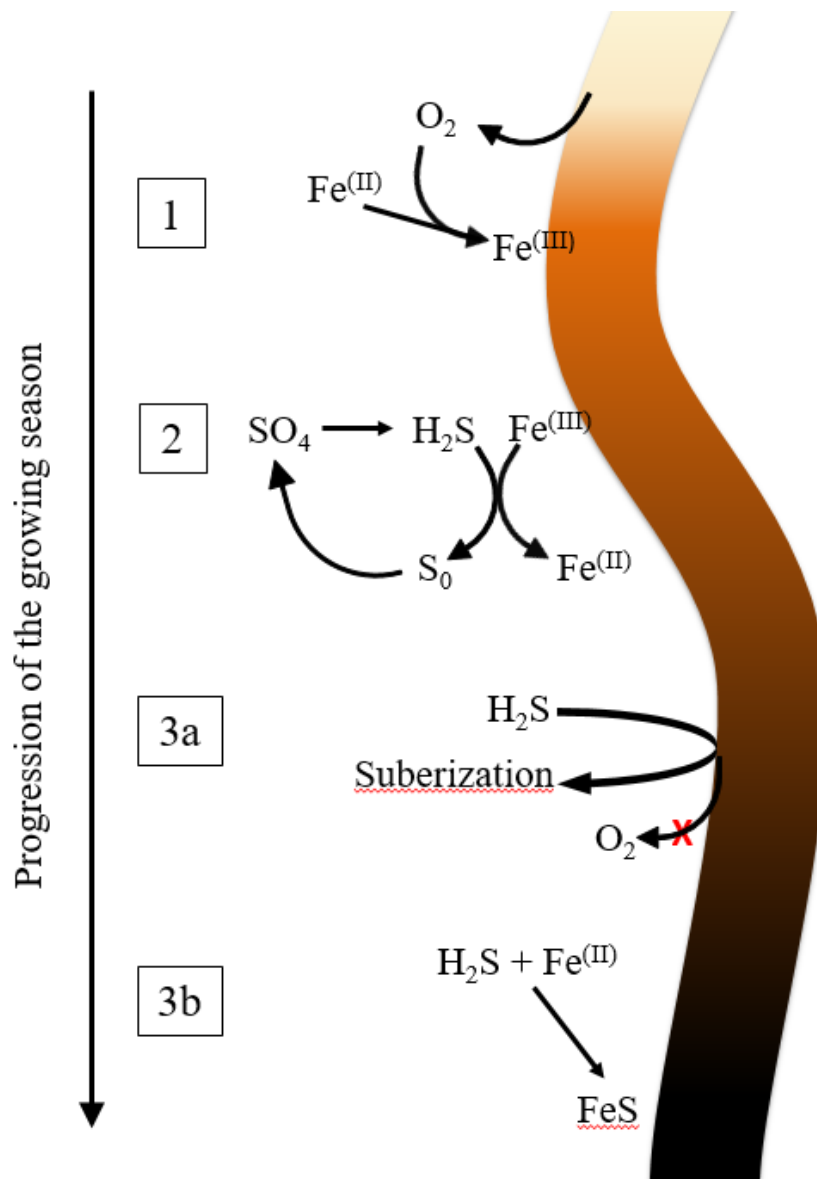


Figure 5. Proposed mechanism of iron sulfide formation on wild rice roots. Roots are protected by iron (hydr)oxides [1], but reduced by sulfide [2]. Exposure of roots to sulfide induces suberization of root cells, which leads to decreased radial oxygen loss [3a]. Rhizosphere anoxia allows iron sulfides to precipitate [3b].

A hypothesized pathway for how the rice roots might transition from iron (hydr)oxide plaques to iron sulfide plaques over the growing season is outlined in Figure 5. Initially, radial oxygen loss creates oxic conditions in the rooting zone, causing ferrous iron within the rhizosphere to precipitate as iron (hydr)oxides and accumulate on root surfaces (Fig. 5, [1] label). At this initial stage, the root is protected from reduced species by both radial oxygen loss and iron (hydr)oxide plaques, an electron accepting sink. Before sulfide can penetrate to the root, the iron (hydr)oxide plaques, effectively acting as an electron accepting buffer, must be reduced (Fig. 5, [2] label). As sulfide erodes the accumulated ferric iron barrier (Hansel et al. 2014, Kwon et al. 2013), sulfide can then reach the root surface and cause suberization (Fig. 5, [3a] label). Once radial oxygen loss is suppressed by suberin formation, the electron accepting buffer capacity of iron (hydr)oxides can no longer be replenished. The remaining quantity of iron (hydr)oxides can be more rapidly reduced due to a net change in the flow of electrons to the rooting zone. Upon depletion of iron (hydr)oxides, sulfide accumulates rapidly, since neither iron (hydr)oxides or a supply of radial oxygen loss are available to oxidize sulfide (Fig 5, [3b] label). As sulfide penetrates closer to the root surface, it precipitates with available iron, and the redox potential of the rhizosphere shifts to more reducing conditions.

The rapid accumulation of sulfur on roots in amended plants seems inconsistent with the relatively small difference in sulfur and iron concentrations in pore water. The saturation index (SI), which is calculated from pore water concentrations two centimeters from the stem, indicates that the pore water is undersaturated with respect to iron sulfide. The thermodynamic understanding of mineral precipitation and dissolution is that minerals precipitate when pore water is saturated and dissolve when pore waters are undersaturated (Stumm & Morgan, 1995). The rapid accumulation of iron sulfide on roots in the setting of undersaturated pore water suggests that the transition of iron (hydr)oxide to iron sulfide on the roots occurs very close to the surface of the root, and thus depends on near-root-surface processes more than on pore water concentrations. Sulfide on root surfaces must be supplied externally, either from reduction of surface water sulfate, or from mobilization of AVS on sediment, but ferrous iron in the FeS plaques could be sourced from the reduction of iron (hydr)oxides already accumulated on

the root surface earlier in the season. Indeed, a decrease in solid-phase iron on the roots, a shift in iron speciation, and an accumulation of pore water iron all occur simultaneously, which is consistent with loss of soluble ferrous iron off of the root surface during the redox transition. Thus, if the ferrous iron in FeS plaques is sourced from the iron (hydr)oxides on the root, saturation index calculations based on pore water iron concentrations may not be relevant to understanding FeS formation on roots. Additionally, the decline of pore water sulfate followed by rapid accumulation of AVS on the root surfaces suggests that a large amount of sulfur passes through the pore water pool very quickly. Iron sulfide formation is strongly favorable thermodynamically and kinetically rapid (Rickard, 1995). Using pore water sulfide concentrations to calculate the saturation index may underestimate the amount of sulfur available to precipitate on root surfaces, as pore water sulfide may act as a transient phase between pore water sulfate and root AVS. The transience of sulfide in pore waters near rice rhizospheres was noted by Hara (2013) who observed black iron sulfide zones around white rice seeds grown in sulfate-amended sediment, but was unable to quantify any sulfide, despite measuring redox potentials low enough to support sulfide production.

In this experiment, iron sulfide plaques occurred concomitantly with lower seed nitrogen and fewer seeds. Less nitrogen was present in the total seed mass of the amended plants, and fewer seeds were produced. This is likely a strategy for optimizing reproduction; amended plants produce fewer filled seeds but each filled seed is fully viable (Pastor et al., in review). The two-component isotope mixing model suggests that the amended plants were not able to compensate for inhibition of nitrogen uptake by translocating a greater percentage of seed nitrogen from the stem and leaves. Between the sulfate and control, no difference was observed in the fraction of N uptake from the pore water. The decreased total seed N in sulfate amended plants appears to be an equally proportioned result of decreased uptake from pore water and decreased translocation from the plant.

Biological variables were only affected during seed production. During the biomass growth life stages, little difference in total plant weight and total plant N was observed. Biomass may not have been impacted because sulfide can produce a fertilization effect by sequestering iron bound with phosphate, releasing free phosphate

(Geurts et al. 2009, Caraco et al. 1989, Smolders et al. 2003, Lamers et al. 2002).

However, nitrogen, rather than phosphorus, is the limiting nutrient for wild rice (Sims et al. 2012), so the fertilization effect is likely minimal in wild rice. In the long term, Pastor et al. (in review) showed that sulfide takes several years to affect a population of wild rice, because although sulfide showed no effect on germination and very little effect on biomass of wild rice, sulfide greatly decreased the number of juvenile seedlings that survive and the number of filled seeds produced by the plant. The results from our study suggest that during seed production, the buffering capacity of iron (hydr)oxides has been overwhelmed by sulfide and no longer protects the plant from sulfide. Similarly, juvenile seedlings may be vulnerable to sulfide because they have not yet grown out of the water column and are thus unable to transport oxygen from the atmosphere to their roots. The life stages of wild rice affected by sulfide are consistent with times during which an oxic barrier around the roots is absent.

Accumulation of FeS on roots may have implications for wetland cycling of iron and sulfide. After senescence, roots coated with FeS decay and become incorporated into the bulk sediment. Jacq et al. (1991) observed significant accumulation of FeS on white rice roots after senescence, likely because the dead root material stimulated continued iron and sulfate reduction. Additionally, Jacq et al. (1991) found that sediment in a planted rice paddy contained higher FeS concentrations than an unplanted rice paddy. Because wild rice is an annual plant, the amount of root FeS that accumulates over a growing season is added to the sediment each year. Choi et al. (2006) likewise found that in a riparian wetland containing *Phragmites australis* and *Zizania latifolia*, AVS concentrations were higher in the top 6 cm of non-vegetated sediment, but vegetated sediment had higher concentrations of AVS 6-14 cm below the sediment-water interface. If AVS on roots is supplied mainly from reduction of surface water sulfate, burial of FeS coated roots may be supplying sulfide to the sediment faster than pore water precipitation of iron sulfide in the bulk sediment. If root AVS is supplied largely by mobilization of sediment AVS, which Choi et al. suggests can be caused by radial oxygen loss, then sediment AVS concentration may be an important parameter in determining iron sulfide accumulation and concomitant inhibition of nitrogen uptake in wild rice. Knowledge of

the main sources of sulfur for root AVS will be crucial in managing wild rice in sulfur-impacted systems.

Conclusion & Directions for Future Work

The timing of our observations of rhizosphere AVS accumulation in conjunction with decreased total seed N in sulfate-amended plants suggests that nitrogen uptake by wild rice is affected only after significant sulfide accumulation on root surfaces. In this experiment, elevated sulfide on plant roots coincides with the plant's reproductive stage. We propose that root surface iron (hydr)oxides delay sulfide from entering the plant, effectively acting as a buffer against early and mid-season sulfide exposure. When the oxic barrier on the root surface is overwhelmed, iron sulfide accumulates rapidly, as shown by the doubling of AVS and the shift in iron speciation from about 50% Fe(II) to 90% Fe(II) within just one week. In this experiment, the oxic barrier was overwhelmed just prior to seed production; concurrently, reduced seed count, total seed weight, and total seed nitrogen were observed.

Many questions remain about the cause of the redox shift in the rhizosphere. We propose a mechanism in which sulfide-induced suberization of roots facilitates reduction of the oxic barrier, but a seasonal change in wild rice physiology could also facilitate a rapid transition to anoxia. Control roots, like sulfate-amended roots, lost about half of their total extractable iron at the start of seed production, and accumulated some ferrous iron even in the absence of significant S accumulation. Is there a seasonal shift in redox potential in wild rice rhizospheres, regardless of the presence of sulfur? Seasonal measurements of redox potential and magnitude of radial oxygen loss may provide insight into the comparative influence of plant processes and sulfur loading on shifting redox conditions in the rhizosphere. Is the bacterial community affected more by rhizosphere geochemistry or by life stages of the plant? Seasonal microbial community analysis could also elucidate the relative causes of the rhizosphere anoxia, as a significant seasonal shift in the microbial community of control plants would indicate plant controlled redox conditions. If the redox conditions of the rhizosphere are controlled by iron and sulfur geochemistry as proposed, would a lower initial concentration of iron on roots result in erosion of the iron (hydr)oxide barrier and subsequent inhibition of nitrogen uptake earlier in the growing season? If so, would plant biomass and nitrogen

also be decreased? A similar study to this one could be done in which total iron concentrations of the sediment were varied to produce different initial concentrations of iron (hydr)oxides on roots.

Finally, from a management perspective, it would be useful to understand the sources of sulfur on root surfaces and the sediment parameters that control those sources. Is the sulfide on the roots sourced primarily from surface water sulfate or from mobilization of sediment AVS? Could a lake that has previously received high sulfur loads but currently has low surface water sulfate contain wild rice with significant iron sulfide plaques? This question has implications for restoration of wild rice in sulfur-impacted lakes.

References

- Allam, A.I., and Hollis, J.P. 1972, "Sulfide inhibition of oxidases in rice roots", *Phytopathology*, vol. 62, pp. 634-639.
- Armstrong, J., AfreenZobayed, F. & Armstrong, W. 1996, "Phragmites die-back: Sulphide- and acetic acid-induced bud and root death, lignifications, and blockages within aeration and vascular systems", *New Phytologist*, vol. 134, no. 4, pp. 601-614.
- Armstrong, J. & Armstrong, W. 2005, "Rice: Sulfide-induced barriers to root radial oxygen loss, Fe²⁺ and water uptake, and lateral root emergence", *Annals of Botany*, vol. 96, no. 4, pp. 625-638.
- Beck, B.F. & Johnson, N.W. 2014, "Geochemical factors influencing the production and transport of methylmercury in St. Louis River Estuary sediment", *Applied Geochemistry*, vol. 51, pp. 44-54.
- Brouwer, H. & Murphy, T. 1994, "Diffusion Method for the Determination of Acid-Volatile Sulfides (Avs) in Sediment", *Environmental Toxicology and Chemistry*, vol. 13, no. 8, pp. 1273-1275.
- Boudreau, B. P. *Diagenetic Models and their Implementation: Modeling Transport and Reactions in Aquatic Sediments*; Springer: New York, 1996.
- Burton, E.D., Sullivan, L.A., Bush, R.T., Johnston, S.G. & Keene, A.F. 2008, "A simple and inexpensive chromium-reducible sulfur method for acid-sulfate soils", *Applied Geochemistry*, vol. 23, no. 9, pp. 2759-2766.
- Caracao, N.F., Cole, J.J., and Likens, G.E. 1989. "Evidence for sulphate-controlled phosphorus release from sediments of aquatic systems", *Letters to Nature*, vol 341, pp. 316-318.
- Choi, J., Park, S. & Jaffe, P. 2006, "The effect of emergent macrophytes on the dynamics of sulfur species and trace metals in wetland sediments", *Environmental Pollution*, vol. 140, no. 2, pp. 286-293.
- Christensen, K. & Sand-Jensen, K. 1998, "Precipitated iron and manganese plaques restrict root uptake of phosphorus in *Lobelia dortmanna*", *Canadian Journal of Botany-Revue Canadienne De Botanique*, vol. 76, no. 12, pp. 2158-2163.
- Eaton, A.D., L.S. Clesceri, E.W. Rice, A.E. Greenberg, eds. 2005, Standard Methods for the Examination of Water and Wastewater, 21st ed. American Public Health Association.

- Eimers, M. C., Dillon, P.J., Schiff, S.L., Jeffries, D.S. 2003. "The effects of drying and re-wetting and increased temperature on sulphate release from upland and wetland material", *Soil Biology and Biochemistry*, vol. 35, no. 12, pp. 1663–1673
- Gao, S., Tanji K.K., and Scardaci, S.C. 2003, "Incorporating straw may induce sulfide toxicity in paddy rice", *California Agriculture* vol. 57, pp. 55-59
- Geurts, J.J.M., Sarneel, J.M., Willers, B.J.C., Roelofs, J.G.M., Verhoeven, J.T.A. & Lamers, L.P.M. 2009, "Interacting effects of sulphate pollution, sulphide toxicity and eutrophication on vegetation development in fens: A mesocosm experiment", *Environmental Pollution*, vol. 157, no. 7, pp. 2072-2081.
- Grava, J. and Raisanen, K.A. 1978, "Growth and nutrient accumulation and distribution in wild rice", *Agronomy Journal* vol 70, pp. 1077-1081.
- Hansel, C.M., Lentini, C.J., Tang, Y., Johnston, D.T., Wankel, S.D. & Jardine, P.M. 2015, "Dominance of sulfur-fueled iron oxide reduction in low-sulfate freshwater sediments", *Isme Journal*, vol. 9, no. 11, pp. 2400-2412.
- Hara, Y. 2013, "Suppressive effect of sulfate on establishment of rice seedlings in submerged soil may be due to sulfide generation around the seeds", *Plant Production Science*, vol 16, no. 1, pp. 50-60.
- Holmer, M and S. Nielsen. 1997, "Sediment sulfur dynamics related to biomass-density patterns in *Zostera marina* (eelgrass) beds", *Marine Ecology Progress Series* vol. 146, pp.163-171.
- Jacq, V.A., Prade, K., and Ottow, J.C.G. 1991, "Iron sulphide accumulation in the rhizosphere of wetland rice (*Oryza sativa* L.) as the result of microbial activities", in *Diversity of Environmental Biogeochemistry* (ed. J. Berthelin) pp. 453-468.
- Jorgenson, K.D., Lee, P.F. & Kanavillil, N. 2013, "Ecological relationships of wild rice, *Zizania* spp. 11. Electron microscopy study of iron plaques on the roots of northern wild rice (*Zizania palustris*)", *Botany*, vol. 91, no. 3, pp. 189-201.
- Joshi, M.M., Ibrahim, I.K.A., and Hollis, J.P. 1975, "Hydrogen sulfide: effects on the physiology of rice plants and relation to straighthead disease", *Phytopathology*, vol 65, pp. 1165-1170.
- Koch, M.S., and Mendelssohn, I.A. 1989, "Sulphide as a soil phototoxin: differential responses in two marsh species", *British Ecological Society*, vol 77, no. 2, pp.565-578.
- Koch, M.S., Mendelssohn, I.A., and McKee, K.L. 1990 "Mechanism for the hydrogen sulfide-induced growth limitation in wetland macrophytes", *Limnology and Oceanography*, vol. 35, no. 2, pp. 399-408.

- Krishnamurthy, P., Ranathunge, K., Franke, R., Prakash, H.S., Schreiber, L. & Mathew, M.K. 2009, "The role of root apoplastic transport barriers in salt tolerance of rice (*Oryza sativa* L.)", *Planta*, vol. 230, no. 1, pp. 119-134.
- Kwon, M.J., Boyanov, M.I., Antonopoulos, D.A., Brulc, J.M., Johnston, E.R., Skinner, K.A., Kemner, K.M. & O'Loughlin, E.J. 2014, "Effects of dissimilatory sulfate reduction on Fe-III (hydr)oxide reduction and microbial community development", *Geochimica et Cosmochimica Acta*, vol. 129, pp. 177-190.
- Lamers, L.P.M., Govers, L.L., Janssen, I.C.J.M., Geurts, J.J.M., Van der Welle, M.E.W., Van Katwijk, M.M., Van der Heide, T., Roelofs, J.G.M. & Smolders, A.J.P. 2013, "Sulfide as a soil phytotoxin-a review", *Frontiers in Plant Science*, vol. 4, pp. UNSP 268.
- Lamers, L., Falla, S., Samborska, E., van Dulken, L., van Hengstum, G. & Roelofs, J. 2002, "Factors controlling the extent of eutrophication and toxicity in sulfate-polluted freshwater wetlands", *Limnology and Oceanography*, vol. 47, no. 2, pp. 585-593.
- Lee, P. & McNaughton, K. 2004, "Macrophyte induced microchemical changes in the water column of a northern Boreal Lake", *Hydrobiologia*, vol. 522, no. 1-3, pp. 207-220.
- Lee, K., and Dunton, K.H. 2000, "Diurnal changes in pore water sulfide concentrations in the seagrass *Thalassia testudinum* beds: the effects of seagrasses on sulfide dynamics", *Journal of Experimental Marine Biology and Ecology*, vol 255, pp. 201-214.
- Martin, N.M. & Maricle, B.R. 2015, "Species-specific enzymatic tolerance of sulfide toxicity in plant roots", *Plant Physiology and Biochemistry*, vol. 88, pp. 36-41.
- Mendelsohn, I., Kleiss, B. & Wakeley, J. 1995, "Factors Controlling the Formation of Oxidized Root Channels - a Review", *Wetlands*, vol. 15, no. 1, pp. 37-46.
- Mendelsohn, I.A., and Postek, M.T. 1982, "Elemental analysis of deposits on the roots of *Spartina alterniflora* Loisel.", *American Journal of Botany* vol 69, no. 6, pp. 904-912.
- Minnesota Pollution Control Agency. 2014. Analysis of the Wild Rice Sulfate Standard Study: Draft for Scientific Peer Review.
- Moyle, J. 1944. Wild rice in Minnesota. *Journal of Wildlife Management* 8:177-184.
- Neubauer, S.C., Toledo-Duran, G.E., Emerson, D. & Megonigal, J.P. 2007, "Returning to their roots: Iron-oxidizing bacteria enhance short-term plaque formation in the wetland-plant rhizosphere", *Geomicrobiology Journal*, vol. 24, no. 1, pp. 65-73.

- Rickard, D. 1995, "Kinetics of FeS Precipitation, Part 1. Competing Reaction Mechanisms", *Geochimica et Cosmochimica Acta* vol. 59, no. 21, pp. 4367-4379.
- Ruiz-Halpern, S., Macko, S.A. & Fourqurean, J.W. 2008, "The effects of manipulation of sedimentary iron and organic matter on sediment biogeochemistry and seagrasses in a subtropical carbonate environment", *Biogeochemistry*, vol. 87, no. 2, pp. 113-126.
- Schmidt, H., Eickhorst, T. & Tippkoetter, R. 2011, "Monitoring of root growth and redox conditions in paddy soil rhizotrons by redox electrodes and image analysis", *Plant and Soil*, vol. 341, no. 1-2, pp. 221-232.
- Seeberg-Elverfeldt, J., Koelling, M., Schluter, M. & Feseker, T. 2005, "Rhizon in situ sampler (RISS) for pore water sampling from aquatic sediments", *Abstracts of Papers of the American Chemical Society*, vol. 230, pp. U1763-U1764.
- Smolders, A., Lamers, L., den Hartog, C. & Roelofs, J. 2003, "Mechanisms involved in the decline of *Stratiotes aloides* L. in The Netherlands: sulphate as a key variable", *Hydrobiologia*, vol. 506, no. 1-3, pp. 603-610.
- Smolders, A. & Roelofs, J. 1996, "The roles of internal iron hydroxide precipitation, sulphide toxicity and oxidizing ability in the survival of *Stratiotes aloides* roots at different iron concentrations in sediment pore water", *New Phytologist*, vol. 133, no. 2, pp. 253-260.
- Snowden, R. & Wheeler, B. 1995, "Chemical changes in selected wetland plant species with increasing Fe supply, with specific reference to root precipitates and Fe tolerance", *New Phytologist*, vol. 131, no. 4, pp. 503-520.
- Soukup, A., Armstrong, W., Schreiber, L., Franke, R. & Votrubova, O. 2007, "Apoplastic barriers to radial oxygen loss and solute penetration: a chemical and functional comparison of the exodermis of two wetland species, *Phragmites australis* and *Glyceria maxima*", *New Phytologist*, vol. 173, no. 2, pp. 264-278.
- St Cyr, L., Fortin, D. & Campbell, P. 1993, "Microscopic Observations of the Iron Plaque of a Submerged Aquatic Plant (*Vallisneria-Americana michx*)", *Aquatic Botany*, vol. 46, no. 2, pp. 155-167.
- Stumm, W., and Morgan, J.J. 1995, *Aquatic Chemistry*, 3rd edition.
- Sun, M., Xiao, T., Ning, Z., Xiao, E. & Sun, W. 2015, "Microbial community analysis in rice paddy soils irrigated by acid mine drainage contaminated water", *Applied Microbiology and Biotechnology*, vol. 99, no. 6, pp. 2911-2922.

- Thamdrup, B., Fossing, H., & Jorgenson, B.B. 1994, "Manganese, iron, and sulfur cycling in a coastal marine sediment, Aarhus Bay, Denmark", *Geochimica et Cosmochimica Acta*, vol. 58, no. 23, pp. 5115-5129.
- VanCappellen, P. V., Wang, Y. 1996. "Cycling of iron and manganese in surficial sediments", *Am. J. Sci.* vol. 296, pp. 197-243.
- Wang, M., Glass, A., Shaff, J. & Kochian, L. 1994, "Ammonium Uptake by Rice Roots .3. Electrophysiology", *Plant Physiology*, vol. 104, no. 3, pp. 899-906.

Appendix

Table 1. Average and standard deviation of the saturation index of FeS in sulfate amended and control pore waters. The K_{sp} value used was $10^{-2.95}$.

Date (julian)	Sulfate-amended	Control
177	-1.436 ± 0.228	-1.436 ± 0.228
190	-0.282 ± 0.346	-0.175 ± 0.354
203	-0.390 ± 0.189	-1.061 ± 0.204
232	-0.560 ± 0.195	-0.802 ± 0.242
239	0.099 ± 0.969	-0.232 ± 0.435
245	-0.140 ± 0.580	-0.410 ± 0.837
256	-0.302 ± 0.376	-0.365 ± 0.333
263	-0.199 ± 0.198	-0.597 ± 0.581



Figure 1. Sulfate-amended root (left) and control root (right). Sulfate-amended root has black color extending from about 0.5 cm above the root ball down to the tips of the roots (not shown). Control root has amber color characteristic of iron (hydr)oxides, especially 2-3 cm below root ball.

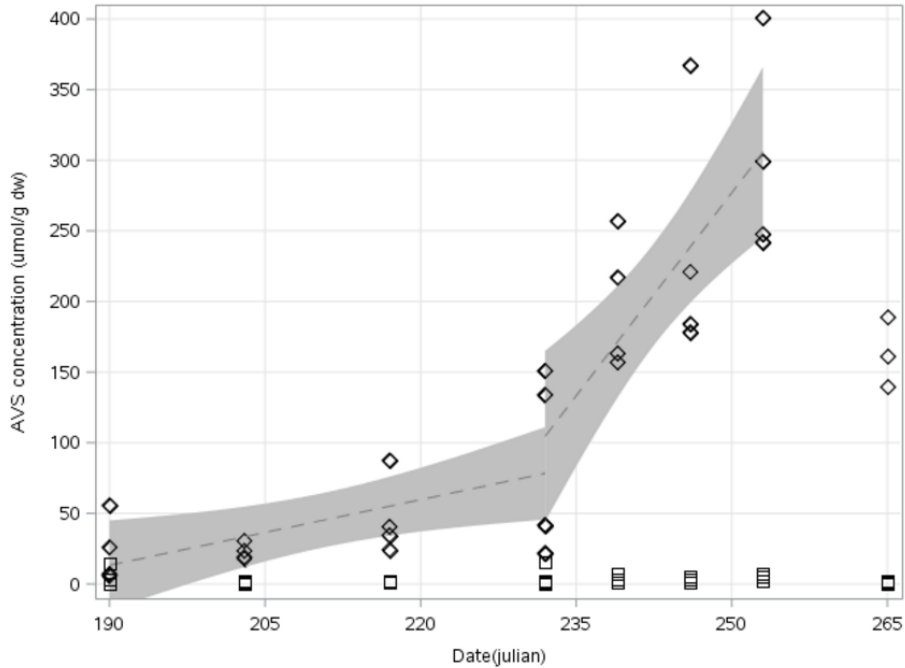


Figure 2. A 95% confidence interval around a regression of time and AVS on sulfate amended roots depicting the change in rate of sulfide accumulation. Diamonds represent sulfate amended plants, and squares represent control plants. The plant is in the flowering stage until day 232, when it starts producing seeds. The last sample date was during senescence, and is therefore not included in the 95% confidence interval.

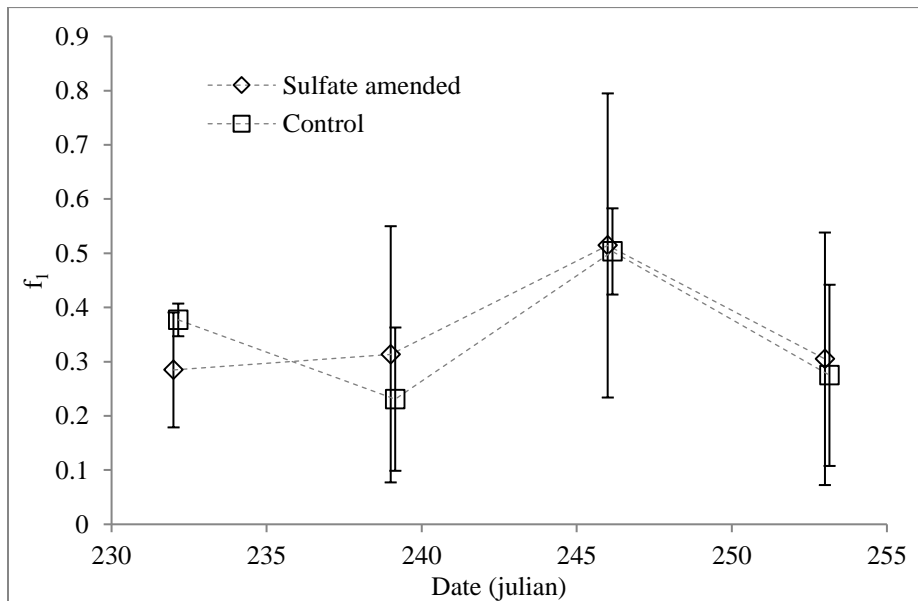


Figure 3. Isotopic mixing model showing the proportion (f_1) of $\delta^{15}\text{N}$ in seeds that originated from ammonium in the pore water during seed production. Diamonds represent sulfate amended plants, and squares represent control plants. Each data point is the average of four replicates. Error bars are one standard deviation.